Journal of Molecular Catalysis A: Chemical 308 (2009) 108–113

Contents lists available at ScienceDirect

Journal of Molecular Catalysis A: Chemical

journal homepage: www.elsevier.com/locate/molcata

Utilization of immobilized biomimetic iron complexes within nanoreactors of Al-MCM-41 as cyclohexane oxidation catalyst

F. Farzaneh[a,*], M. Poorkhosravani[a,b], M. Ghandi[b]

[a] Department of Chemistry, University of Alzahra, Vanak, Tehran, Iran
[b] School of Chemistry, University College of Science, University of Tehran, Tehran, Iran

ARTICLE INFO

Article history:
Received 16 January 2009
Received in revised form 19 March 2009
Accepted 20 March 2009
Available online 19 April 2009

Keywords:
Iron complexes
Al-MCM-41
Cyclohexane
Oxidation

ABSTRACT

Biomimetic iron(III) complexes such as $[Fe(en)_2Cl_2]Cl$, $[Fe(bpy)_2Cl_2]Cl$, [Fe(salen)Cl], [Fe(TPP)Cl] and [Fe(TMC)Cl] in which en, bpy, salen, TMC, and TPP refer to ethylenediamine, 2,2′-bipyridine, N,N′-bis(salicylidene)ethylenediamine), 5,7,12,14-tetramethyl-1,4,8,11 tetraazacyclotetradeca 4,6,11,13-tetraene and meso-tetraphenylporphyrin were immobilized within nanoreactors of Al-MCM-41. The structures of immobilized complexes were characterized by powder X-ray diffraction (XRD), nitrogen adsorption–desorption, FTIR and UV–vis spectroscopy. The pore volume, surface area and pore diameter of Al-MCM-41 were found to decrease after immobilization of iron complexes. It was found that immobilized iron complexes within Al-MCM-41 with the order of $[Fe(bpy)_2Cl_2] > [Fe(TPP)Cl] > [Fe(TMC)Cl] \sim [Fe(salen)Cl] > [Fe(en)_2Cl_2]Cl$ catalyze the oxidation of cyclohexane to cyclohexanol and cyclohexanone with hydrogen peroxide in refluxing acetonitrile.

1. Introduction

Catalytic oxidation of C–H bond in saturated hydrocarbons under mild conditions is a key step in the oxyfunctionalization of organic compounds [1,2]. Among the various metals, iron is the most abundant metal in nature and is indispensable species of nearly all organisms. Nature has evolved a number of metalloenzymes such as the heme-containing cytochrome P450 and the nonhem monooxygenase. Many biological systems such as hemoglobin, myoglobin, cytochrome oxygenases are iron containing enzymes or co-enzymes [3,4]. There has been significant interest in modeling of the aforementioned enzyme active sites and developing the biomimetic oxidation catalysts. Therefore, many attempts have been made to synthesize the iron complexes with bipyridines [5,6], polypyridines [7,8], phtalocyanines [9], porphyrines [10–15], salens [16,17] and macrocyclic ligands [7]. Transition metalocomplexes either encapsulated or grafted within microporous (zeolites) or mesoporous materials (MCMs) [18–23] as inorganic mimics of hybrid materials have received special attentions. In these materials, the supporting media acts as protein in comparison to that of metalloenzymes [18,24]. They have numerous potential applications such as catalysts, photocatalysts, and gas sensors.

In this study, we have immobilized $[Fe(en)_2Cl_2]Cl$, $[Fe(bpy)_2Cl_2]Cl$, [Fe(salen)Cl], [Fe(TPP)Cl] and [Fe(TMC)Cl] within Al-MCM-41 nanoreactors in order to investigate their catalytic activity on cyclohexane oxidation with the green oxidant hydrogen peroxide.

2. Experimental

2.1. Materials

All materials were of commercial reagent grade. Iron (III) chloride, cetyltrimethylammoniumbromide [CTAB), tetraethylorthosilicate, aluminumisopropoxide (%99), tetraethylammonium hydroxide solution (10% in water), ethylenediamine, 2,2′-bipyridine, acetone, diethyl ether, salicylaldehyde, acetylacetone, tert-butyl alcohol, pyrrole, propionic acid, benzaldehyde, dimethylformamide, methanol, ethanol, acetonitrile, H_2O_2 (30%), cyclohexane, cyclopentane, diphenylamine and DMF were purchased from Merck Chemical Company and used without further purification.

2.2. Characterization

BET surface areas and pore size distributions of initially degassed samples at 373 K for 90–120 min were calculated from nitrogen adsorption–desorption isotherms obtained at 77 K with a Belsorp Mini-II instrument. The UV–vis measurements were performed on a double beam UV–vis PerkinElmer Lambda 35 spectrophotometer. X-ray diffraction patterns were obtained by a Siefert 3003 PTS

* Corresponding author. Tel.: +98 21 88258977; fax: +98 21 66495291.
E-mail address: farzaneh@alzahra.ac.ir (F. Farzaneh).

1381-1169/$ – see front matter © 2009 Elsevier B.V. All rights reserved.
doi:10.1016/j.molcata.2009.03.039

diffractometer using Cu Kα radiation (λ = 1.5406 Å). FTIR spectra were recorded with a Bruker Tensor 27 IR spectrometer in KBr pellets over the range of 400–4000 cm^{-1} under the atmospheric conditions. The amount of iron complexes immobilized within nanoreactors of Al-MCM-41 was determined by atomic absorption spectroscopy (AAS) with a GBC spectrophotometer using flame approach, after HF acid dissolution. Cyclic voltammetry (CV) was performed using a Metrohm computerized Voltammetric analyzer model 746 VA stand with the glassy carbon disc working electrode (WE) (1.8 mm diameter) and platinum wire as the counter electrode (CE). The WE potentials were measured versus the 3 M KCl Ag/AgCl reference electrode. All electrodes were obtained from Metrohm. Oxidation products were analyzed by GC and GC Mass using Agilent 6890 Series, with FID detector, HP-5, 5% phenylmethylsiloxane capillary and Agilent 5973 Network, mass selective detector, HP-5 MS 6989 Network GC system, respectively.

2.3. Synthesis

2.3.1. Synthesis of Al-MCM-41

The Al-MCM-41 (Si/Al = 30) was prepared according to the reported method [24]. Tetraethylorthosilicate (22.3 ml, 1 mol) was added to a mixture of aluminum isopropoxide (0.68 g, 0.033 mol) in deionized water (5 ml). The mixture was stirred for 30 min at a speed of about 250 rpm and tetraethylammonium hydroxide solution (0.4 ml, 10% water) was added with continuous stirring for another 30 min until a gel was formed (pH 11). Cetyltrimethylammonium bromide (7.2 g, 0.2 mol in 60 ml deionized water) was then added dropwise (30 ml/h) until the gel was changed into a suspension. The suspension was transferred into a teflon-lined steel autoclave and heated to 150 °C for 48 h. After cooling to room temperature, the product was separated by filtration, washed with deionized water and ethanol, dried in air at 100 °C for 1 h and finally calcined under the flowing air at 540 °C for 6 h.

2.3.2. Preparation of the complexes

2.3.2.1. Preparation of [Fe(bpy)$_2$Cl$_2$]Cl. [Fe(bpy)$_2$Cl$_2$]Cl was prepared according to the modified reported method [25]. $FeCl_3$ (0.16 g, 1 mmol) was dissolved in ethanol (10 ml) and 2,2′-bipyridine (0.312 g, 2 mmol) was added to this solution. The resultant solution which turned into dark orange upon addition of the ligand, was refluxed for 15 min while stirring until the complex formation was appeared. After cooling to room temperature, diethyl ether (30 ml) was added, and the precipitate was then filtered, washed with a mixture of acetone and diethyl ether (1:6, vol/vol) and dried at room temperature. The IR and UV–vis spectra were identical with those reported previously [26,27].

FT-IR: 3062, 3106, 1600, 1441, 1000–1200, 768 cm^{-1}.

UV–vis: λ_{max} at 275, 360, 510 nm.

2.3.2.2. Preparation of [Fe(en)$_2$Cl$_2$]Cl. The aforementioned procedure was used for the preparation of [Fe(en)$_2$Cl$_2$]Cl. Ethylendiamine (0.66 ml, 3 M solution in ethanol) was added dropwise to $FeCl_3$ (0.16 g, 1 mmol) in ethanol (10 ml). The solution was then stirred for 30 min. After cooling to room temperature, the precipitate was filtered, washed with ethanol and dried at room temperature.

FT-IR: 2975, 2910, 1600, 1085 cm^{-1}.

UV–vis: λ_{max} at 270, 335 nm.

2.3.2.3. Preparation of [Fe(salen)Cl]. Salen was synthesized by reaction of ethylendiamine (1 mol) and salicylaldehyde (2 mol) in a methanol (10 ml) in an ice bath. The precipitate was filtrated and washed with cold methanol. The synthesis of Fe(III) salen was carried out according to the reported method [28]. $FeCl_3$ (0.81 g, 0.005 mol in 10 ml ethanol) was added to the a solution of salen (4.02 g, 0.015 mol) in ethanol (140 ml) and the mixture was stirred for 1 h under reflux condition. After cooling to room temperature, the precipitate was filtered, washed with ethanol and dried at room temperature.

FT-IR: 1629, 1597, 1544, 1436, 1370 cm^{-1}.

UV–vis: 235, 265, 300, 320, 500 nm [29,30].

2.3.2.4. Preparation of [Fe(TMC)Cl]. [Fe(TMC)Cl] was synthesized according to the previously reported method [31].

FT-IR: 3195, 1604, 1547, 1436, 1369 cm^{-1} [31].

UV–vis: λ_{max} at 320, 480 nm [32].

2.3.2.5. Preparation of [Fe(TPP)Cl]. [Fe(TPP)Cl] was prepared according to the previously reported procedure [33–35].

FT-IR: 3418, 3023, 1486, 1221, 1312, 1066, 1177, 969, 999, 755, 799, 827, 701 cm^{-1} [36].

UV–vis: 415 nm (Sorbet band), 510 nm [37].

2.3.3. Preparation of catalysts

Al-MCM-41 (1 g) was added to the complex (1.5 mmol in 100 ml ethanol). The mixture was refluxed while stirring for 8 h under nitrogen atmosphere. The solid product was then filtered, and soxhelet extracted with enough amount of absolute ethanol (or a 1:1 mixture of dichlorometane and ethanol in the case of [Fe(TPP)Cl]) in order to remove the weakly adsorbed metallocomplexes on the mesoporous surface. The solids were finally dried in air at room temperature.

2.4. Oxidation reactions

Oxidation reactions were carried out at atmospheric pressure under reflux conditions. Typically a mixture of immobilized iron complex/Al-MCM-41 as catalyst (0.1 g) and cyclohexane (20 mmol dissolved in 5 ml acetonitrile) was added into the reaction flask with slow stirring. After a few minutes, H_2O_2 (24 mmol, 30% aqueous solution), was added and the mixture was refluxed for 8 h. The solid was filtered and washed with fresh acetonitrile. The filtrate solution was then subjected to GC and GC Mass analysis.

3. Result and discussion

3.1. Characterization of Al-MCM-41 and immobilized iron complex/Al-MCM-41

3.1.1. XRD studies

The XRD patterns of Al-MCM-41 (Fig. 1a), which exhibits a strong peak at $2\theta = 1.7$ for the ⟨1 0 0⟩ reflection and two weak and broad peaks at $2\theta = 3.00$ and $2\theta = 3.6$, respectively, for the ⟨1 1 0⟩, ⟨2 0 0⟩ reflections, is consistent with that reported before [24]. All reflections can be indexed on a hexagonal lattice. The XRD of the immobilized iron complexes/Al-MCM-41 are presented in Fig. 1b–g. No evidence of collapsed Al-MCM-41 structure is observed with the exception of reduction in the peak intensities due to complex immobilization [38–41].

3.2. Nitrogen adsorption–desorption studies

The nitrogen adsorption–desorption isotherm plots for Al-MCM-41 and immobilized iron complexes/Al-MCM-41 are given in Fig. 2. The type IV isotherms [23] indicates that adsorption takes place as a thin layer on the walls at low relative pressures (P/P_0) (monolayer coverage). Sharp inflections at 0.4–0.3 for Al-MCM-41 and immobilized iron complexes are related to the capillary condensation and confirm the existence of uniform pores. In addition, the inflection heights of iron complexes in nitrogen adsorption isotherm plots are smaller than that of Al-MCM-41. It is attributed to

Table 1
Texture parameters of samples taken from nitrogen adsorption–desorption and atomic adsorption studies.

Solid	BET specific surface area ($m^2\,g^{-1}$)	Total pore volume ($ml\,g^{-1}$)	Average pore diameter (nm)	d value (Å)	Lattice parameter[a] (Å)	% Fe
Al-MCM-41	661.14	1.0385	6.2831	59.04	68.25	–
Fe(III)/Al-MCM-41	643.77	1.1023	6.849	59.44	68.71	0.89
$[Fe(bpy)_2Cl_2]^+$/Al-MCM-41	489.88	0.9113	7.4407	59.83	69.16	1.55
[Fe(TPP)Cl]/Al-MCM-41	527.7	0.9304	7.0528	58.86	68.04	0.60
[Fe(TMC)Cl]/Al-MCM-41	629.21	1.0154	6.4551	58.52	67.64	0.70
[Fe(salen)Cl]/Al-MCM-41	557.37	0.9263	6.6479	57.76	66.77	3.68
$[Fe(en)_2Cl_2]^+$/Al-MCM-41	621.96	1.0911	7.0172	57.66	66.65	2.92

[a] Determined by equation $a_0 = d_{100}(2/3^{1/2})$.

the reduced pore volume, which reflects the surface area decreasing (Fig. 2 and Table 1). This effect can be attributed to the iron complex inclusions into the Al-MCM-41 pores. The iron percentages present in the immobilized complexes/Al-MCM-41 are presented in Table 1. As is observed in Table 1, the amount of iron depends on the complex type.

3.3. FTIR studies of immobilized iron complexes within Al-MCM-41

The FTIR spectra of immobilized iron complexes/Al-MCM-41 are given in Table 2. The 450–1200 cm^{-1} range is dominated by the framework vibration of Al-MCM-41 in all samples [24]. In addition, the band at 1630 cm^{-1} is due to the bending vibration of H_2O in Al-MCM-41. Regardless of this, the bands attributed to aromatics and ligand C=N and C=C vibrations of immobilized complexes appear at 1602–1400 cm^{-1} region.

3.4. Study of catalytic activity of various immobilized iron complexes

In a preliminary investigation, the effect of time was examined on the oxidation reaction in the presence of $[Fe(bpy)_2Cl_2]^+$/Al-MCM-41 as catalyst. As seen in Fig. 3, 74% of cyclohexane is converted to cyclohexanol and cyclohexanone during 14 h. Comparison of the results during 8 and 14 h exhibited in Fig. 3 shows that although increasing time increases the cyclohexane conversion from 60 to 74%, no improvement is observed in cyclohexanol and cyclohexanone yields. Furthermore, it was found that utilization of 0.1 g of catalyst provides the maximum cyclohexane conversion during 8 h (Fig. 4).

Effect of Fe(III) complexes/Al-MCM-41 (0.1 g) as catalysts were studied on cyclohexane oxidation during 8 h. The results are pre-

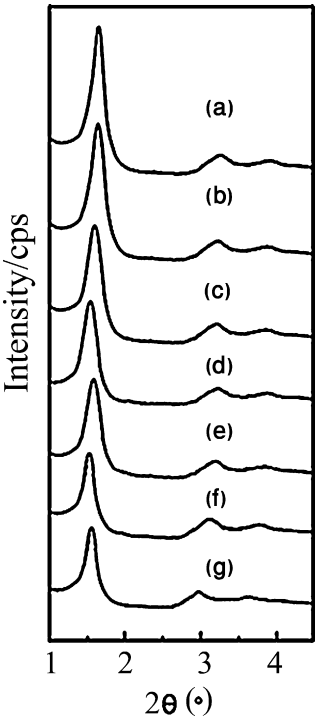

Fig. 1. X-ray diffraction patterns of (a) calcined Al-MCM-41, (b) Fe(III)/Al-MCM-41, (c) $[Fe(bpy)_2Cl_2]^+$/Al-MCM-41, (d) [Fe(TMC)Cl]/Al-MCM-41, (e) [Fe(TPP)Cl]/Al-MCM-41, (f) [Fe(salen)Cl]/Al-MCM-41, and (g) $[Fe(en)_2\ Cl_2]^+$/Al-MCM-41.

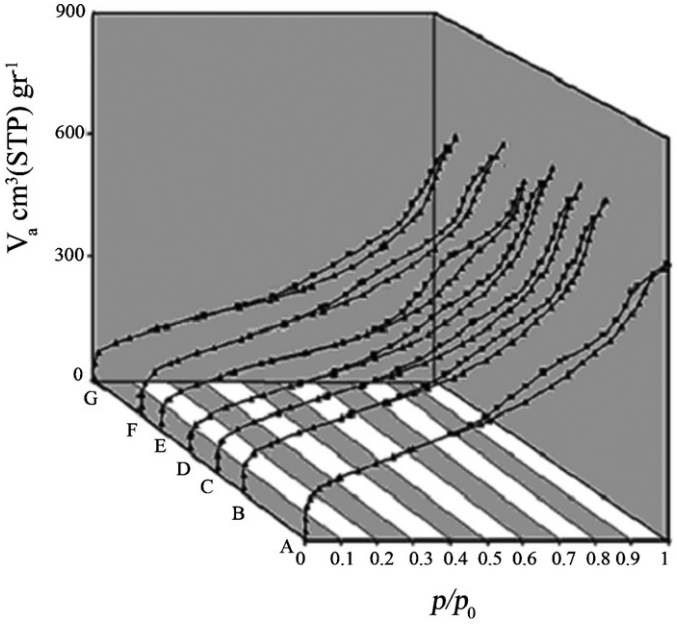

Fig. 2. Nitrogen adsorption–desorption isotherms of (a) Al-MCM-4, (b) Fe(III)/Al-MCM-41, (c) $[Fe(en)_2Cl_2]^+$/Al-MCM-41, (d) $[Fe(bpy)_2Cl_2]^+$/Al-MCM-41, (e) [Fe(salen)Cl]/Al-MCM-41, (f) [Fe(TMC)Cl]/Al-MCM-41, and (g) [Fe(TPP)Cl]/Al-MCM-41.

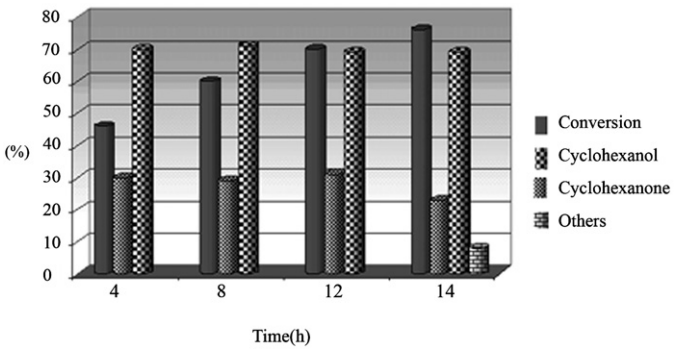

Fig. 3. Effect of time on cyclohexane oxidation with H_2O_2 catalyzed by $[Fe(bpy)_2Cl_2]^+$/Al-MCM-41.

Table 2
FTIR data of Fe(III) complex/Al-MCM-41.

Catalyst	Si–OH (cm^{-1})	Si–O–Si (cm^{-1})			C=N (cm^{-1})	C=C (cm^{-1})
		Asy.	Sym.	Ben.		
Al-MCM-41	3414	1079	806	459	–	–
Fe(III)/Al-MCM-41	3440	1095	808	466	–	–
$[Fe(en)_2Cl_2]^+$/Al-MCM-41	3422	1085	812	465	–	–
$[Fe(bpy)_2Cl_2]^+$/Al-MCM-41	3423	1090	808	464	1629	1500
[Fe(TPP)Cl]/Al-MCM-41	3424	1077	800	465	1631	1506
[Fe(TMC)Cl]/Al-MCM-41	3434	1085	810	464	1632	1506
[Fe(salen)Cl]/Al-MCM-41	3421	1077	800	465	1632	1482

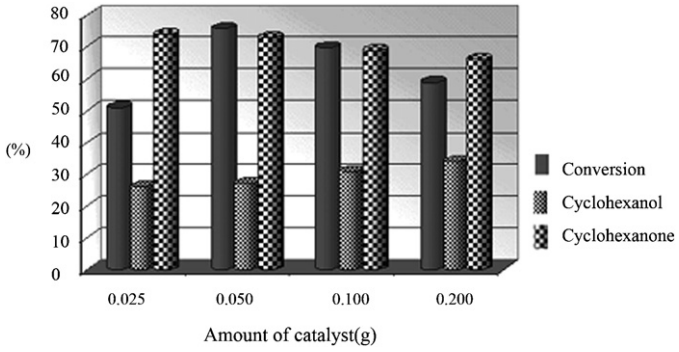

Fig. 4. Effect of the amount of $[Fe(bpy)_2Cl_2]^+$/Al-MCM-41 on cyclohexane conversion.

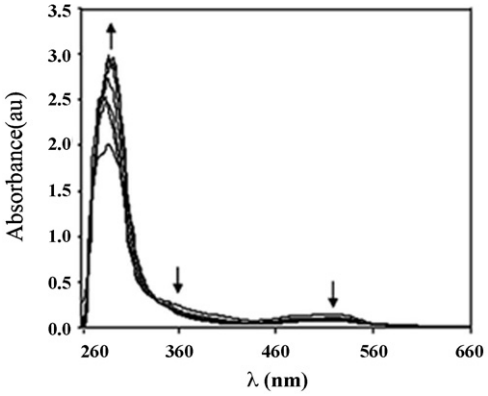

Fig. 6. Titration of $[Fe(bpy)_2Cl_2]$ Cl with H_2O_2, the spectra were recorded after successive addition of one drop H_2O_2 to 1×10^{-4} M solution (10 ml) of $[Fe(bpy)_2Cl_2]Cl$ in CH_3CN.

sented in Table 3. We have included the effect of Al-MCM-41 and Fe(III)/Al-MCM-41 in Table 3 (entries 1 and 2) in order to make the comparisons more convenient. As seen in Table 3, a substantial amount of cyclohexane (60%) has been converted to cyclohexanol and cyclohexanone in the presence of $[Fe(bpy)_2Cl_2]^+$/Al-MCM-41 as catalyst for oxygen transfer from H_2O_2 to cyclohexane. Particularly significant is the selectivity observed toward the formation of cyclohexanol and cyclohexanone as the sole detectable products. Obtaining the similar oxidation results when the reaction was carried out either in the presence of air or under nitrogen atmosphere clearly excluded the effect of oxygen atmosphere on the oxidation processes. Compared to the results obtained in the presence of Fe(III)/Al-MCM-41 which showed about 3% cyclohexane conversion (Table 3, entry 2), observation of 60% cyclohexane oxidation with the TON of 650 in the presence of immobilized $[Fe(pby)_2Cl_2]^+$/Al-MCM-41 provides the key role of immobilized bipyridine ligands complexed to Fe(III) within the Al-MCM-41 nanoreactors. Although [Fe(TPP)Cl] (Table 3, entry 6) showed moderate activity and highest TON, our later studies revealed about 10% catalyst desorption during the oxidation reaction.

The UV–vis spectra of $[Fe(pby)_2Cl_2]Cl$, $[Fe(pby)_2Cl_2]^+$/Al-MCM-41 and Al-MCM-41 in ethanol are exhibited in Fig. 5. The spectrum of $[Fe(pby)_2Cl_2]Cl$ in ethanol solution displays three bands at 275, 360 and 510 nm. The band at 275 nm with $\varepsilon = 1.0 \times 10^4$ dcm^3 mol^{-1} cm^{-1} is assigned to an interligand transition characteristic of pyridine compounds [42]. The band at 510 nm with low intensity is unambiguously attributed to $P\pi$–Fe^{III} $d\pi$ ligand metal charge transfer (LMCT). The presence of Fe^{III}–Cl bond as well leads to LMCT involving chloride $p\pi$–$d\pi$ orbitals. Observing bands at UV region and a broad band at visible region might be attributed to the presence of complex within Al-MCM-41 nanoreactors (Fig. 5b).

In order to establish the possible reaction pathway, H_2O_2 (30% aqueous solution) in acetonitrile was added dropwise to a solution of 1×10^{-4} M of $[Fe(pby)_2Cl_2]Cl$ in acetonitrile and the progress of reaction was monitored by UV–vis absorption spectroscopy (Fig. 6). A decrease in the bands appear at 360 and 510 nm with concomitant increase in the band appears at 275 nm occur with marginal shift to a longer wavelength. On the basis of these results, the implication of an oxo iron species arising from the interaction of H_2O_2 with iron complex might be concluded [38]. This species in turn is responsible for oxygen transfer to cyclohexane leading to cyclohexanone and cyclohexanol.

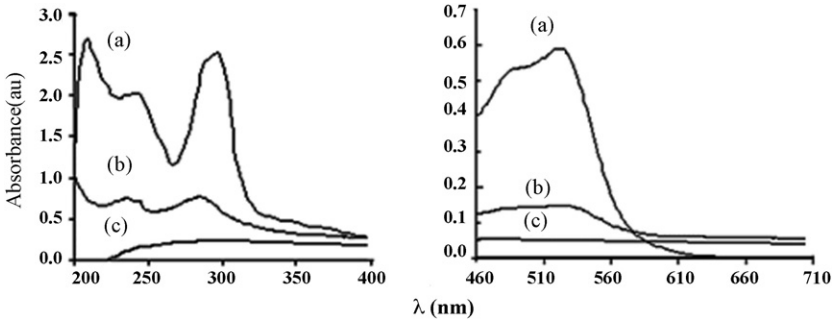

Fig. 5. UV–vis spectra of (a) $[Fe(bpy)_2Cl_2]$ Cl, (b) $[Fe(bpy)_2Cl_2]^+$/Al-MCM-41, (c) Al-MCM-41 in ethanol.

Table 3
Result of cyclohexane oxidation with H_2O_2 (30%)[a] in the presence of heterogeneous Iron(III) complexes.

Entry	Catalyst	Conversion (%)	ol (%)	one (%)	TON[b]
1	Al-MCM-41	–	–	–	–
2	Fe(III)/Al-MCM-41	3	24	76	54
3	$[Fe(en)_2Cl_2]^+$/Al-MCM-41	14	10	90	78
4	[Fe(salen)Cl]/Al-MCM-41	18	35	65	78
5	[Fe(TMC)Cl]/Al-MCM-41	19	21	79	430
6	[Fe(TPP)Cl]/Al-MCM-41	42	34	66	1120[c]
7	$[Fe(bpy)_2Cl_2]^+$/Al-MCM-41[d]	60	29	71	650
8	$[Fe(bpy)_2Cl_2]^+$/Al-MCM-41[e]	90	18	82	1011
9	$[Fe(bpy)_2Cl_2]$/Al-MCM-41	28	12	88	571
10	$[Fe(bpy)_2Cl_2]Cl$[f,g]	72	27	56	686

[a] 20 mmol.
[b] mmol of products/mmol of iron complex.
[c] 10% desorption of catalyst was observed.
[d] After reaction completion, the catalyst after separation and washing exhibited about 40% conversion with similar selectivities in a new run.
[e] 36 mmol oh H_2O_2 was used.
[f] Homogeneous catalyst.
[g] 17% of unidentified products were observed.

The iron complexes showed a distinct redox couple in the cyclic voltamogram which is attributed to Fe^{+3}/Fe^{+2} transition. The $E_{1/2}$ value of this couple for $[Fe(en)_2Cl_2]Cl$ and $[Fe(bpy)_2Cl_2]Cl$ were determined to be 1.20 (irreversible), and 0.12, respectively. Observation of the least and the most catalytic reactivities respectively for the two immobilized complexes (see Table 3) containing the comparable diamine ligands, with maximum and the minimum amount of $E_{1/2}$ is a logical anticipation.

To rationalize the reaction mechanism, the implication of the putative $[(L_n)Fe(III)=O]$ intermediate seems a likely pathway. Such a proposal is taken from Fe(III) catalyzed oxyfunctionalization of saturated hydrocarbons and cyclic ethers with hydrogen peroxide by Barton and ourselves [43,44]. In the first step, interaction of H_2O_2 with the catalyst produces an activated Fe(V)=O species. This drives from the heterolytic breakage of the O–O bond in hydrogen peroxide, and is responsible for the activation of hydrocarbon by generating a monosubstituded alkyl derivative. In the second step, the dioxygen produced by H_2O_2 generates the alkyl hydroperoxide via insertion into the carbon-iron bond. Subsequent reduction or fragmentation affords cyclohexanol and cyclohexanone, respectively. That cyclohexanone is partly generated through oxidation of cyclohexanol to cyclohexanone by dioxygen generated *in situ* from H_2O_2 was realized when the oxidation reaction was carried out in the presence of H_2O_2 in excess amount. As seen in Table 3, entry 8, an increase in cyclohexane conversion (from 60 to 90%) concomitant with a decrease and an increase respectively in cyclohexanol (from 29 to 18%) and cyclohexanone (from 71 to 82%) yields might be a likely route to the formation of cyclohexanone in higher percentage yield.

4. Conclusions

The immobilized iron complexes within nanoreactors of Al-MCM-41 were prepared and characterized. Catalytic activities of these complexes have been tested for the oxidation of cyclohexane with H_2O_2. It was shown that the Al-MCM-41 nanoreactors is a suitable medium for immobilization of large biomimetic molecules. With the exception of [Fe(TPP)Cl]/Al-MCM-41), no desorption was detected during the course of reactions.

Acknowledgment

This study was financially supported by Research Council of the University of Alzahra.

References

[1] A.E. Shilov, G.B. Shulpin, Chem. Rev. 97 (1997) 2879.
[2] U. Schuchardt, D. Cardoso, R. Sercheli, R. Pereira, R.S. da Cruz, M.C. Guerreiro, D. Mandelli, E.V. Spinace, E.L. Pires, Appl. Catal. A: Gen. 211 (2001) 1.
[3] A.D.N. Vaz, D.F. McGinnity, M.J. Coon, Proc. Natl. Acad. Sci. U.S.A. 95 (1998) 3555.
[4] F.P. Guengerich, T.L. Macdonald, FASEB J. 4 (1990) 2453–2459.
[5] N.M.F. Carvalho, A. Horn Jr., O.A.C. Antunes, Appl. Catal. A: Gen. 305 (2006) 140.
[6] G.V. Nizova, B. Krebs, G. Suss-Fink, S. Schindler, L. Westerheide, L.G. Cuervo, G.B. Shulpin, Tetrahedron 58 (2002) 9231.
[7] M. Costas, K. Chen, L. Que Jr., Coord. Chem. Rev. 200–202 (2000) 517.
[8] C. Hemmert, A.P. Maestrin, M. Renz, H. Gornitzka, B.C.R. Meunier, Acad. Sci. Paris, Serie IIc, Chim./Chem. 3 (2000) 735.
[9] N. Grootboom, T. Nyokong, J. Mol. Catal. A: Chem. 179 (2002) 113.
[10] W.-D. Woggon, Acc. Chem. Res. 38 (2005) 127.
[11] Y. Miyazaki, A. Satake, Y. Kobuke, J. Mol. Catal. A: Chem. 283 (2008) 129.
[12] M.H.N. Olsen, G.C. Salomao, V. Drago, C. Fernandes, A. Horn Jr., L. Cardoz Filho, O.A.C. Antunes, J. Supercrit. Fluids 34 (2005) 119.
[13] W. Nam, H.J. Lee, S.-Y. Oh, C. Kim, H.G. Jang, J. Inorg. Biochem. 80 (2000) 219.
[14] Y. Terazono, D. Dolphin, Inorg. Chim. Acta 346 (2003) 261.
[15] C.C. Guo, M.-F. Chu, Q. Liu, Y. Liu, D.-C. Guo, X-.Q. Liu, Appl. Catal. A: Gen. 246 (2003) 303.
[16] G.C. Salomao, M.H.N. Olsen, V. Drago, C. Fernandes, L. Cardozo Filho, O.A.C. Antunes, Catal. Commun. 8 (2007) 69.
[17] A. Haikarainen, J. Sipila, P. Pietikainen, A. Pajunen, I. Mutikainen, Bioorg. Med. Chem. 9 (2001) 1633.
[18] J. Połtowicz, K. Pamin, E. Tabor, J. Haber, A. Adamski, Z. Sojka, Appl. Catal. A: Gen. 299 (2006) 235.
[19] I.L. Viana Rosa, C.M.C.P. Manso, O.A. Serra, Y. Iamamoto, J. Mol. Catal. A: Chem. 160 (2000) 199.
[20] A. Fuerte, A. Corma, M. Iglesias, E. Morales, F. Sanchez, J. Mol. Catal. A: Chem. 246 (2006) 109.
[21] V.R. Rani, M.R. Kishan, S.J. Kulkarni, K.V. Raghavan, Catal. Commun. 6 (2005) 531.
[22] B.T. Holland, C. Walkup, A. Stein, J. Phys. Chem. B 102 (1998) 4301.
[23] J. Haber, K. Pamin, J. Połtowicz, J. Mol. Catal. A: Chem. 224 (2004) 153.
[24] M. Selvaraj, A. Pandurangan, K.S. Seshadri, P.K. Sinha, V. Krishnasamy, K.B. Lal, J. Mol. Catal. A: Chem. 192 (2003) 153.
[25] M.N. Collomb, A. Deronzier, K. Gorgy, J.C. Lepreütre, J. Pecaut, New J. Chem. (1999) 785.
[26] P.P. Knops-Gerrits, C.A. Trujillo, B.Z. Zhan, X.Y. Li, p. Rouxhet, P.A. Jacobs, Topics Catal. 3 (1996) 437.
[27] D. Bhattacharyya, S. Chakraborty, P. Munshi, G.K. Lahiri, Polyhedron 18 (1999) 2951.
[28] G.C. Salomao, M.H.N. Olsen, V. Drago, C. Fernandes, L.C. Filho, O.A.C. Antunes, Catal. Commun. 8 (2007) 69.
[29] H. Hamdan, V. Navijanti, H. Nur, M.N.M. Muhid, Solid State Sci. 7 (2005) 239.
[30] M. Izakovic, J. Sima, Acta Chim. Slov. 51 (2004) 427–436.
[31] J.C. Medina, N. Gabriunas, E. Páez-Mozo, J. Mol. Catal. A: Chem. 115 (1997) 233–239.
[32] X. Hu, K. Mayr, Inorg. Chim. Acta 337 (2002) 53.
[33] A.D. Adler, F.R. Longo, J.D. Finarelli, J. Goldmacher, J. Assour, L. Korsakoff, J. Org. Chem. 32 (1967) 476.
[34] A.D. Longo, F.R. Longo, F. Rampas, J. Kim, J. Inorg. Nucl. Chem. 32 (1970) 2443.
[35] A.A. Costa, G.F. Ghesti, J.L. de Macedo, V.S. Braga, M.M. Santos, J.A. Dias, S.C.L. Dias, J. Mol. Catal. A: Chem. 282 (2008) 149.
[36] G. Fagadar-Cosma, V. Badea, D.V. Lascici, E. Fagadar-Cosma, M. Simon, The 13th Symposium on Analytical and Environmental Problems, Szeged, 25 September, 2006.

[37] M.H.N. Olsen, M.F.M. Lopes, G.C. Salomao, C. Fernandes, A. Horn Jr, L. Cardozo Filho, O.A.C. Antunes, 2nd Mercosur Congress on Chemical Engineering 4th, Mercosur Congress on Process Systems Engineering (2005), (www.enpromer2005.eq.ufrj.br/nukleo/pdfs/0223_enpromer_olsen_and_lopes_2005.pdf).
[38] M.R. Maurya, A.K. Chandrakar, S. Chand, J. Mol. Catal. A: Chem. 274 (2007) 192.
[39] M. Masteri-Farahani, F. Farzaneh, M. Ghandi, Catal. Commun. 8 (2007) 6.
[40] P. Oliveira, A. Machado, A.M. Ramos, I. Fonseca, F.M. Braz Fernandes, A.M. Botelho do Rego, J. Vital, Micropor. Mesopor. Mater. 120 (2009) 432.
[41] T. Yokoi, T. Tatsumi, H. Yoshitake, J. Colloid Interface Sci. 274 (2004) 451.
[42] M. Lubben, A. Meetsma, F. Bolhuis, B.L. Feringa, Inorg. Chim. Acta 215 (1994) 123.
[43] D.H.R. Barton, S.D. Beviere, W. Chavasiri, E. Csuhai, D. Doller, Tetrahedron 48 (14) (1992) 2895.
[44] M. Salavati Niassary, F. Farzaneh, M. Ghandi, J. Mol. Catal. A: Chem. 175 (2001) 105.